IEEE Access
Multidisciplinary ⋮ Rapid Review ⋮ Open Access Journal

Received 1 July 2023, accepted 16 July 2023, date of publication 20 July 2023, date of current version 31 July 2023.

Digital Object Identifier 10.1109/ACCESS.2023.3297511

RESEARCH ARTICLE

Road Recognition and Stability Control for Unmanned Ground Vehicles on Complex Terrain

XIANG AO[1], LI-MING WANG[1], JIA-XIN HOU[1], YU-QUAN XUE[1], SHANG-JUN RAO[1], ZI-YANG ZHOU[1], FU-XUE JIA[1], ZHI-YUAN ZHANG[2], AND LONG-MEI LI[1]

[1]School of Electrical Engineering, Naval University of Engineering, Wuhan, Hubei 430034, China
[2]School of Power Engineering, Naval University of Engineering, Wuhan, Hubei 430034, China

Corresponding author: Long-Mei Li (vivianlee527@163.com)

This work was supported by the Hubei Provincial Natural Science Foundation under Grant 2022CFB865.

ABSTRACT The study of unmanned ground vehicles (UGVs) operating under unstructured roads is of great significance to intelligent transportation, agricultural development and military technology. In order to ensure reliable and stable operation of UGVs on unstructured terrain, it is necessary to identify the current road terrain and perform vehicle stability adjustment. Road terrain identification is a prerequisite for stability control. Most of the existing road terrain identification methods use a single vehicle sensor, which has the problem that complex algorithms need to be applied for data processing, which reduces the real-time performance. Moreover, the single sensor is weak in anti-interference and limited in recognizing the road. To address these problems, a method is proposed to collect vehicle motion data using on-board gyroscope sensors and velocity sensors. Back propagation (BP) neural network is used to identify the category of the road. For the problem that the conventional proportional-integral differential (PID) algorithm cannot be adapted to different road stability control, a multi-loop adaptive proportional-integral differential (PID) control system with the velocity loop as the outer loop and the torque (current) loop as the inner loop is proposed. In order to verify the feasibility and effectiveness of the method, experiments are conducted on a UGV using robot operating system (ROS), and the results verify the feasibility and superiority of the road identification and stability control method proposed in this paper. It provides a good theoretical basis and valuable technical guidance for the UGV operation and control on unstructured roads.

INDEX TERMS Adaptive algorithms, BP neural networks, complex terrain, multi-loop PID control systems, road identification.

I. INTRODUCTION

Unmanned Ground Vehicles (UGVs) are mobile ground robots that are crucial components of intelligent transportation systems and a significant research area in ground mobile robotics. They have diverse applications in fields such as military, agriculture, and aerospace [1], [2], [3], [4], [5], [6]. Ensuring the stable operation of UGVs requires careful consideration of road recognition and stability control, which are two critical factors. Road recognition is a particularly significant research area for UGVs and has attracted widespread interest. Roads are commonly classified as structured or unstructured, with the latter being more challenging to study due to their complex terrains, varying undulations, and the difficulty in establishing reasonable mathematical models [7], [8], [9].

Extensive research has been conducted by numerous scholars and experts on the recognition of unstructured road terrain for UGVs, which can be classified into three main categories. The first category, as proposed by Sun Yu-ze, involves acquiring original remote sensing map images using software such as BIGEMAP, decomposing the image into ground information and elevation data, and processing them through neural network algorithms [10]. A grid map is produced by combining these data, completing macroscopic road terrain recognition. It is clear that the first category is well-suited for the creation of macroscopic maps through the extraction of road terrain information with the aid of diverse mapping

The associate editor coordinating the review of this manuscript and approving it for publication was Zahid Akhtar.

This work is licensed under a Creative Commons Attribution-NonCommercial-NoDerivatives 4.0 License.
For more information, see https://creativecommons.org/licenses/by-nc-nd/4.0/

projection software. Nevertheless, it lacks the utilization of sensors for real-time information extraction, finally leading to a certain level of latency. The second category relies on external vehicle sensors, such as LiDAR or depth cameras, for real-time Simultaneous Localization and Mapping (SLAM). A semantic SLAM system is presented by Zhang et al. [11], which constructs semantic maps utilizing entities and incorporates them into an RGB-D SLAM framework. Imani et al. provides a precise perceptual review of SLAM case histories that rely on laser/ultrasonic sensors and cameras as input data [12]. Two methods for constructing SLAM are proposed by Lemaire et al. [13], one employing stereo vision and the other utilizing monocular images. This kind of method is mainly applied to the detection of rocks and trees in the outdoors, but the external sensor is easily affected by the environment (humidity, light intensity, water reflection), so it is not good at identifying microscopic terrain features, such as road topography, road surface roughness. The third category involves recording vehicular travel data through internal sensors such as Inertial Measurement Units (IMUs) or velocity sensors. This type of method is more suitable for dealing with microscopic information of roads, so the road identification method studied in this paper belongs to this category.

The method proposed by Zhen [14] is road recognition based on pitch angle information. This method is characterized by using a single sensor for road detection, which can effectively reduce costs. It has a good recognition result. However, the information provided by a single sensor is limited, and the anti-interference is weak. Some time-consuming complex data processing method (such as KNN algorithm, singular value decomposition, clustering algorithm et al.) must be used to integrate the sensor extraction to form better input features, resulting in poor real-time performance. Similarly, Brooks et al. [15] adopted a single vibration sensor for road identification, which has the same characteristics as the method proposed by Zhen [14]. Xiaofei et al. [16] adopts road classification based on the correlation between adhesion coefficient and slip coefficient of vehicles driving on the road. The feature of this processing method is that it makes use of its own attributes of road terrain for recognition, which has a wider recognition range and can effectively recognize more road terrain. However, it is difficult to select a suitable sensor for the detection of slip coefficient and adhesion coefficient. Gorges et al. [17] adopts angular velocity sensor and suspension spring elasticity sensor for road recognition. This method can be well applied to two-wheeled motorcycles with obvious suspension spring changes, but it cannot be well applied to vehicles with more than four wheels. At the same time, the sensors selected by these authors are vibration and elastic force sensors, which have a good effect on the road surface with large fluctuation, but the recognition effect on the road surface with small fluctuation and high slip rate (sandy land) is poor. Moreover, the anti-interference of a single sensor is weak, requiring a more complex algorithm to extract data and reduces real-time capability.

Road recognition is the premise of stability control, and the ultimate goal is to ensure the stable control of the unmanned vehicle under different road surfaces.

The importance of UGV stability control research is paramount, in addition to the recognition of unstructured roads. Currently, the research in this domain can be categorized into two groups: model-based control and non-model-based control. According to reference [18], Model Predictive Control (MPC) is a class of algorithms utilized for predictive purposes. These algorithms utilize the vehicle's nonlinear dynamic model to predict the future state of the vehicle during each control cycle. An optimization control problem is solved over a finite time horizon to obtain a control sequence that ultimately leads to optimal control effects. However, on off-road roads, it is difficult to establish a reasonable mathematical model because of the fluctuating road surface, so model control is difficult to achieve. At this time, another type of method can be adopted, i.e., non-model control. Proportional-Integral-Derivative (PID) control is a non-model-based control technique that is widely applicable and robust. A comprehensive control algorithm was designed by Wang et al. [19]to control both yaw and roll motion simultaneously, utilizing the fuzzy PID approach. The fuzzy control proposed in paper [19] is applicable to the unstructured pavement which is difficult to be described. Furthermore, the fuzzy parameter calculation method given in literature [20] can be used as a reference for this paper. Arof et al. [21] proposes a control technique that employs a three-level cascaded Proportional-Integral-Derivative (PID) controller for acceleration and deceleration control in electric vehicles (EVs), using an up-down algorithm to control speed, torque, and position. The speed and torque (current) loops of the three-loop control proposed in the paper [21] can be used as a reference for the control model in this paper, so that the speed and torque of the unmanned vehicle are simultaneously taken into account to ensure the off-road performance of the unmanned vehicle.

In summary, the current study of road recognition for unmanned vehicle is generally based on a single sensor, such as vibration sensors or force sensors. It can reduce part of the cost, but requires some complex methods to process the data sampled by the sensors, which will lead to weak real-time and anti-interference performance. For some slightly undulating but slippery roads (such as sand road), it is difficult to identify. With regard to the stability control of unmanned vehicles, non-model PID control algorithms are commonly used to control the speed and torque of the motor, but a single PID algorithm does not meet the requirements of stable operation of unmanned vehicles under different roads. Therefore, compared with the current research, the novelty of this paper can be summarized as:

(1) Considering the problems of poor real-time, weak anti-interference and limited recognition of roads by a single sensor, this paper proposes to record the shaking information of the unmanned vehicle by sampling the roll angle and pitch

angle under different road surfaces through the gyroscope sensor. The speed information is sampled by the left and right wheel motor speed sensors (motor encoders). The increase in sampling information enhances the system's anti-interference and real-time performance. At the same time, the method is able to calculate the slip state of the unmanned vehicle in real time, allowing for the recognition of more varieties of road terrains.

(2) A control system with a multi-loop adaptive PID algorithm is proposed, which uses the speed loop as the outer loop and the torque loop (current loop) as the inner loop. A fuzzy PID algorithm is used for the speed loop and a segmented PID algorithm is used for the torque loop, which automatically adjusts the PID parameters of both according to the current road properties to achieve stable driving on different roads.

The rest of the paper is organized as follows. Section II gives a detailed description of the theoretical approach to road recognition and stability control of unmanned vehicles. In Section III, experiments on road recognition and stability control of unmanned vehicles are designed to verify the theoretical approach proposed in Section II. Section IV provides a detailed analysis and comparison of the experimental results and illustrates the superiority of the method adopted in this paper. Section V discusses the conclusion and future work. The research flow of this paper is shown in Figure 1.

II. THEORETICAL METHODS

When a UGV operates on complex road surfaces, it is essential to take into account two critical aspects: complex road recognition and stability control.

Road identification is a prerequisite, and suitable PID control parameters are selected for stability control. Stability control is the ultimate goal to ensure the stability of vehicles on different roads.

A. ESTABLISHMENT OF THE VEHICLE MOTION COORDINATE SYSTEM

To effectively extract road information features and establish a reliable control system, a thorough comprehension of the vehicle's motion posture information is indispensable. Therefore, it is essential to establish a rotating coordinate axis for the vehicle.

Figure 2 demonstrates the decomposition of the oscillation information of the vehicle during driving into angular velocities pertaining to the x-axis, y-axis, and z-axis. These correspond to the pitch, roll, and yaw angles, respectively, which are analyzed quantitatively.

B. EXTRACTION OF VEHICLE MOTION INFORMATION

To obtain the vehicle's motion posture information as mentioned above, the gyroscope (IMU) sensor can be utilized. Meanwhile, the vehicle's speed information can be extracted by means of an encoder. This enables the measurement of the vehicle's roll, pitch, and yaw angles, as well as its traveling speed. Such measurements reflect the current road conditions.

C. BUILDING A BP NEURAL NETWORK MODEL

In this study, four common terrain surfaces on which UGVs frequently operate have been selected for feature recognition.

These surfaces include asphalt, short-grass road, tall-grass road, and sandy terrain. Due to the nonlinear relationship between input features and output road results, a BP classification neural network is utilized for feature recognition. The BP neural network model, as depicted in Figure 3, comprises of feature vectors composed of extracted features. The input layer is composed of a feature matrix that contains these feature vectors. The rows of the feature matrix correspond to different types of features, while the columns correspond to the number of extracted features for each type. The input matrix is then fed into the input layer of the BP neural network, and recognition results are generated under the combined action of activation functions in the hidden and output layers. The input feature processing method is discussed in detail in the experimental section.

The theoretical outputs are established for each terrain surface as follows: asphalt surface (1, 0, 0, 0), short grass road surface (0, 1, 0, 0), tall grass road surface (0, 0, 1, 0), and sandy surface (0, 0, 0, 1). The neural network compares the actual output with the theoretical output, calculates the error, and adjusts the weights and thresholds through the network's backpropagation error adjustment function.

D. SELECTION OF ACTIVATION FUNCTION

Sigmoid function is adopted as activation function, as demonstrated by Equation (1). This function has been selected due to its ease of optimization and capability of managing.

high-dimensional data, enabling superior recognition of road attributes. In order to process the data, the input variable parameters are mapped to the range [1, 0] using Equation (1), and subsequently, they are introduced into the neural network.

$$f(x) = \frac{1}{1 + e^{(-x)}} \tag{1}$$

E. ROAD RECOGNITION

To recognize the attributes of the road on which the vehicle is traveling, it is necessary to transform the information obtained by the aforementioned sensors into input features for the BP neural network. The detailed procedure is presented in Figure 4.

After analyzing the feature recognition methods presented in the relevant literature [22], [23], [24], [25], the following observations have been made: when handling data processing, intricate data processing method are necessary to carry out feature processing when the quantity of detected information is meager. On the other hand, when the amount of detected information is large, simple data processing method can be employed for feature processing, and the inclusion of more information can enhance the anti-interference capability of the recognition system. Consequently, multiple pieces

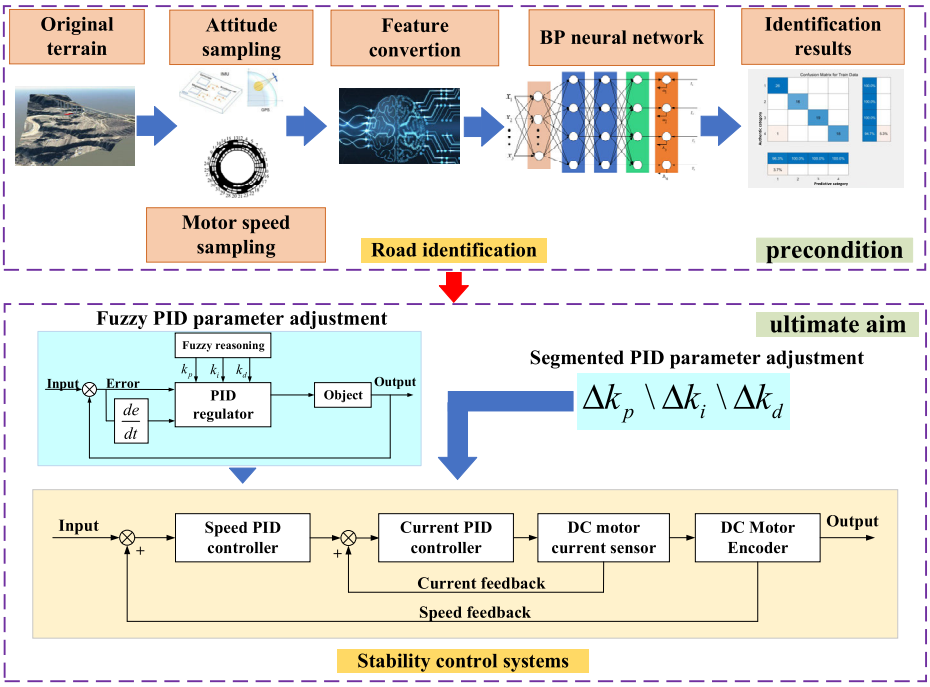

FIGURE 1. The research method of this paper.

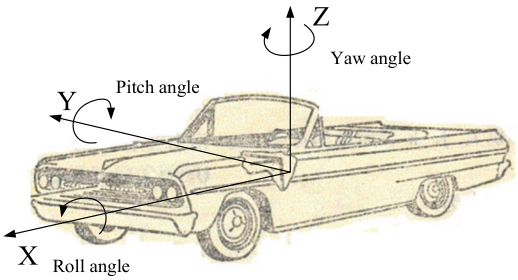

FIGURE 2. Vehicle motion coordinate system.

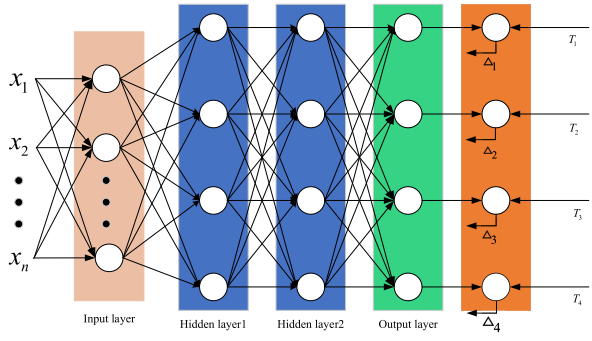

FIGURE 3. BP neural network model.

of information, such as roll angle, pitch angle, and motor speed, have been selected for feature processing. Finally, the processed features are fed into the neural network for recognition.

F. ESTABLISHMENT OF MOTOR MODEL

To achieve better on-board motor control, it is necessary to establish a motor model, as depicted in Figure 5.

In accordance with Kirchhoff's circuit law, the voltage balance equation for the motor can be formulated as follows:

$$U_a = I_a R_a + L_a \frac{di_a}{dt} + E \tag{2}$$

$$E = C_\xi \Phi_c n \tag{3}$$

where C_ξ is torque constant, I_a is armature current, U_a is armature voltage, E is back electromotive force, Φ_c refers to unit magnetic flux, L_a is armature inductance, R_a represents armature resistance.

Since the direct current motor acts as the driving force for intelligent vehicles, the direction of its electromagnetic torque T_a corresponds to the direction of rotational speed n, whereas the load torque T_m and friction torque T_f are in the opposite direction. Utilizing Newton's second law, the torque equation on the motor shaft can be derived as follows:

$$T_a - (T_m + T_f) = J \frac{d\xi}{dt} \tag{4}$$

$$\xi = \frac{2\pi n}{60} \tag{5}$$

Subsequently, the correlation between motor torque and current can be deduced as follows:

$$T_a = T_m + T_f + J(\frac{\pi}{30})\frac{dn}{dt} = C_T \Phi_c I_a = 9.55 C_\xi \Phi_c I_a \tag{6}$$

The relationship between motor speed and armature voltage can be expressed as:

$$n = \frac{U_a}{C_\xi \phi_c} - \frac{R_a T_a}{9.55 C_\xi^2 \phi_c^2} \tag{7}$$

The aforementioned formulas demonstrate that motor torque can be regulated by adjusting the armature current,

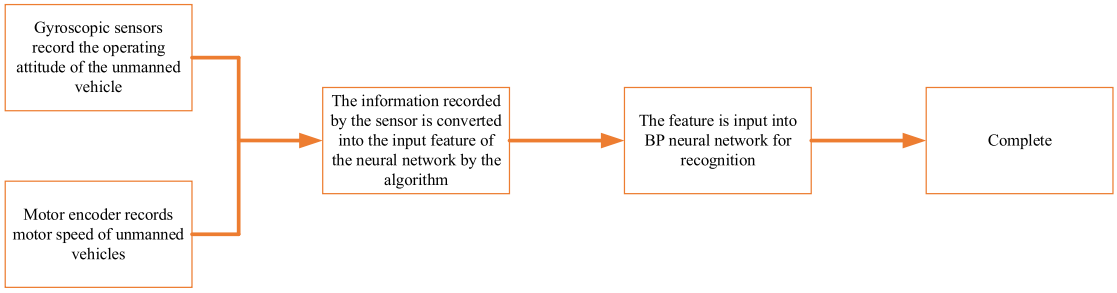

FIGURE 4. Information-to-feature transformation process.

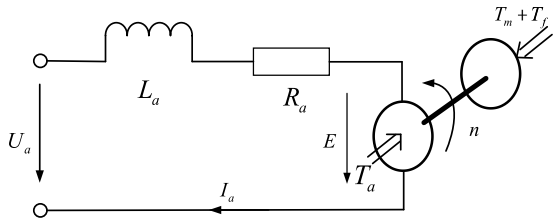

FIGURE 5. Motor model.

while motor speed can be controlled by adjusting the armature voltage. Additionally, motor speed is also influenced by motor torque. Hence, in designing the control system, the first step involves setting the desired speed and subsequently adjusting the armature current to achieve the target speed, thereby setting the motor torque. Finally, the output voltage is regulated to attain the desired speed and target torque. This approach presents a sequence of control for the multi-loop control system, which will be discussed later.

G. ESTABLISHMENT OF THE PID CONTROL SYSTEM

In off-road environments, the primary challenge for implementing vehicle motion control is the instability of control execution caused by the intricate and diverse road scenarios. To address this issue, discrete PID algorithms can be employed for preliminary control, and parameters can be adjusted to suit different tasks. The control equation for this purpose is as follows:

$$u(k) = k_p e(k) + k_i T \sum_{j=0}^{20} e(k) + k_d \frac{e(k) - e(k-1)}{T} \tag{8}$$

By adjusting the values of k_p, k_i, and k_d, the output target value can be adjusted accordingly. Moreover, to ensure the stability of the control system, a cascaded control is employed for the vehicle motor. Based on the aforementioned control strategy, the current loop is configured as the inner loop, while the speed loop serves as the outer loop. This ensures that the current does not experience excessive overshooting, while maintaining a stable motor speed.

H. ESTABLISHMENT OF ADAPTIVE PID CONTROL RULES

Due to the challenge of accurately describing road attributes when the vehicle is operating in off-road environments, an adaptive PID method is utilized to adjust the parameters. Specifically, the speed PID adjustment can be obtained directly from the current speed information obtained through the motor encoder. Given that the speed is continuously changing, a fuzzy PID control method is employed. To accomplish this, the input is set as the error (e), while the change in error is designated as error change(ec). The fuzzy control rules can be expressed as follows:

$$\begin{aligned} k_p &= k_p{}' + \{e_i, ec_i\}_p \\ k_i &= k_i{}' + \{e_i, ec_i\}_i \\ k_d &= k_d{}' + \{e_i, ec_i\}_d \end{aligned} \tag{9}$$

To achieve stable control of motor torque, it is necessary to adapt the current PID control system to the current road attributes. Detection of road attributes is accomplished by means of the BP classification neural network mentioned earlier, yielding discrete changes in results. Consequently, a segmented PID control approach is employed for motor torque regulation. The rules governing this segmented control method are as follows:

$$\begin{aligned} k_p &= k_p' + \Delta k_p \\ k_i &= k_i' + \Delta k_i \\ k_d &= k_d' + \Delta k_d \end{aligned} \tag{10}$$

As a consequence of the foregoing analysis, the adaptive PID control model can be illustrated in Figure 6.

III. EXPERIMENTAL METHOD

A. EXPERIMENTAL DESIGN

To validate the proposed method, a ROS-based UGV is operated on various road surfaces, including asphalt, short grass road, tall grass road, and sandy road surfaces, respectively. The UGV parameters are listed in Table 1.

During the operation, the traveling speeds and attitude angles were recorded to provide relevant data for subsequent feature extraction. The experimental setup is illustrated in Figure 7.

B. FROM SENSOR INFORMATION TO FETURES

The experiments were carried out in accordance with the aforementioned requirements, and the results are presented in Figure 8.

Upon analysis of the changes in both angle and velocity while traversing diverse types of road surfaces by the UGV,

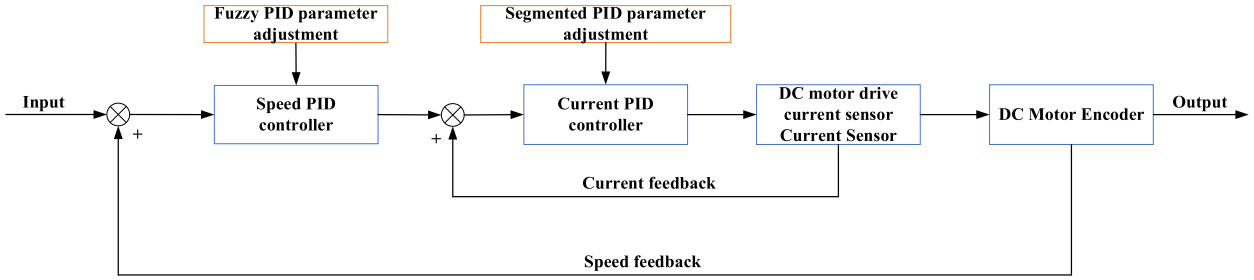

FIGURE 6. Adaptive PID control model diagram.

(a) asphalt road (b) short grass road (c) tall grass road (d) sandy road

FIGURE 7. Experimental road surface.

TABLE 1. Experimental UGV parameter list.

Attribute	Parameters
Self-respect	19.54kg
Maximum speed	1.65m/s
Size	774*570*227mm
Motor	100W DC brushless motor
Wheel material	Rubber
Road category	Asphalt road, short grass road, tall grass road, sandy road
Controller type	main controller: raspberry pie secondary controller: stm32

it is manifest that the divergences are notably substantial. Table 2 presents the subsequent features that can be selected and implemented as inputs for the neural network.

Feature X_1 represents the mean change in pitch angle throughout vehicular operation, wherein $\varphi_{y(k)}$ signifies the pitch angle value at the K-th sampling, and $\varphi_{y(k+1)}$ indicates the pitch angle value at the $K+1$-th sampling. K represents the quantity of samplings. Feature X_2 signifies the mean change in roll angle during vehicular operation, wherein $\varphi_{x(k)}$ represents the roll angle value at the K-th sampling, and $\varphi_{x(k+1)}$ indicates the roll angle value at the $K+1$-th sampling. K constitutes the quantity of samplings. Features X_1 and X_2 serve to document the aggregate oscillation information of the vehicle while traversing the road segment.

Feature X_3 represents the count of abrupt pitch angle changes during vehicular operation, wherein a single pitch angle sudden change is defined as: $\left|\varphi_{y(k+1)} - \varphi_{y(k)}\right| > 5°$. Feature X_4 signifies the count of roll angle sudden changes during vehicular operation, wherein a single roll angle sudden change is defined as: $\left|\varphi_{x(k+1)} - \varphi_{x(k)}\right| > 5°$. Features X_3 and X_4 serve to document the severity of the vehicle's oscillations while traversing the road segment.

Feature X_5 represents the maximal pitch angle difference during vehicular operation, wherein φ_{ymax} signifies the maximal sampled pitch angle value when the vehicle traverses the road, and φ_{ymin} indicates the minimal sampled pitch angle value. Feature X_6 represents the maximal roll angle difference during vehicular operation, wherein φ_{xmax} signifies the maximal sampled roll angle value when the vehicle traverses the road segment, and φ_{xmin} indicates the minimal sampled roll angle value. Features X_5 and X_6 serve to document the maximal oscillation angles on the road segment.

Feature X_7 and Feature X_8 represent the counts of sudden changes in the left wheel motor speed $k_{n_{lv}}$ and the right wheel motor speed $k_{n_{rv}}$, respectively, with a single sudden change in motor speed defined as $|n(k+1) - n(k)| > 100r/min$. Feature X_9 signifies the mean speed disparity between the left and right wheels, wherein $n_{lv}(k)$ represents the K-th sampled speed of the left wheel motor, and $n_{rv}(k)$ indicates the K-th sampled speed of the right wheel motor. K constitutes the quantity of samplings. Feature X_7-X_9 is used to record the motor characteristics of the vehicle.

C. DEFINITION OF INPUT-OUT ADAPTIVE PID DATA SETS

The speed deviation e and the rate of change of speed deviation ec are categorized into nine fuzzy set linguistic variables: " Negative Big (NB)", " Negative Medium (NM)", "Negative Small (NS)", "Negative Less (NL)",

TABLE 2. Feature-information data processing method table.

Serial umber	Feature name	Feature expression
1	Average pitch angle change:	$X_1 = \frac{\sum_{k=1}^{k} \lvert \varphi_{y(k+1)} - \varphi_{y(k)} \rvert}{k}$
2	Average roll angle change:	$X_2 = \frac{\sum_{k=1}^{n} \lvert \varphi_{x(k+1)} - \varphi_{x(k)} \rvert}{k}$
3	Pitch angle sudden change times:	$X_3 = k_{\varphi y}$
4	Change times of roll angle:	$X_4 = k_{\varphi x}$
5	Maximum pitch angle difference	$X_5 = \varphi_{y\max} - \varphi_{y\min}$
6	Maximum roll angle difference	$X_6 = \varphi_{x\max} - \varphi_{x\min}$
7	The number of sudden changes in the rotation speed of the left wheel motor:	$X_7 = k_{n_{lv}}$
8	The number of sudden changes in the speed of the right wheel motor:	$X_8 = k_{n_{rv}}$
9	Average speed difference between left wheel and right wheel	$X_9 = \frac{\sum_{k=1}^{n} \lvert n_{lv}(k) - n_{rv}(k) \rvert}{k}$

"Zero (ZO)", "Positive Less (PL)", "Positive Small (PS)", "Positive Medium (PM)", and "Positive Big (PB)", with domains being $\{-12, -9, -6, -1.8, 0, 1.8, 6, 9, 12\}$, respectively. These variables are applied to the speed loop.

The road attributes are categorized into four categories: "Asphalt Road Surface - Zero (ZO)", "Sandy Road Surface - Negative Small (NS)", "Short Grass Road Surface - Negative Medium (NM)", and "Tall Grass Road Surface - Negative Big (NB)", with increments of $\{0, -10, -15, -20\}$ applied to the current loop.

D. DEFINITION OF FUZZY CONTROL INPUT-OUTPUT MEMBERSHIP FUNCTIONS

To facilitate computation in the speed loop, membership functions are required based on the established domains. Triangular membership functions are employed for fuzzification in this paper. The fuzzy membership functions for e and ec are depicted in Figure 9.

E. ESTABLISHMENT OF ADAPTIVE RULES

According to the mechanical characteristics of the motor and practical experience with the PID algorithm, it has been observed that adjusting the k_p and k_i parameters can accelerate the tuning speed, but such adjustments are likely to cause overshoot effects. Conversely, the k_d parameter can effectively suppress overshoot, but it may slow down the tuning speed. In light of these observations, the recommended approach is to moderately increase the tuning speed on relatively flat surfaces, where the impact on motor output speed and torque is minimal. On uneven surfaces, however, where the impact on motor output speed and torque is substantial, the primary focus should be on suppressing overshoot to enhance system stability. In accordance with the above guidelines, the design of the speed fuzzy control truth table is presented in Table 3, while the current segmented control truth table is presented in Table 4.

Premised on the incremental models outlined in Tables 3 and 4, the tuning of adaptive PID parameters has been completed, effectively achieving the desired control effect.

IV. RESULTS AND DISCUSSION

A. UNSTRUCTURED ROAD RECOGNITION RESULTS

The aforementioned feature information is incorporated into MATLAB's BP classification neural network for recognition

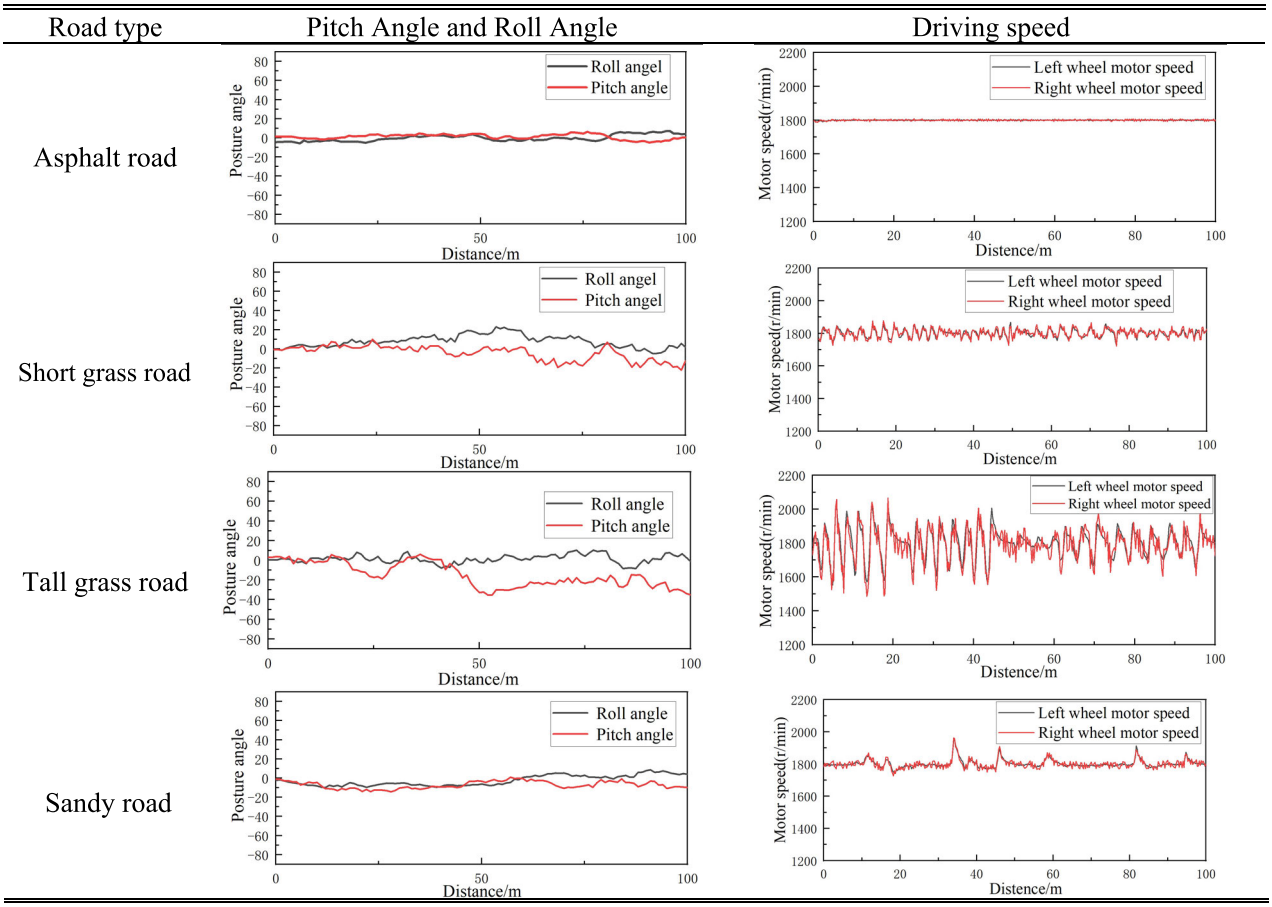

FIGURE 8. Changes in pitch, roll angles, and speed on different road surfaces.

TABLE 3. The truth table of speed in fuzzy PID control.

$k_p/k_i/k_d$	e.								
	NB	NM	NS	NL	ZO	PL	PS	PM	PB
NB	PB/NB/NS	PB/NB/NL	PM/NB/NS	PM/NM/NS	PS/NM/NB	PS/NL/NS	PL/NL/NS	PL/ZO/NM	ZO/ZO/PL
NM	PB/NB/PS	PB/NB/NL	PM/NM/NS	PM/NM/NS	PS/NS/NL	PS/NS/NL	PL/NL/NS	ZO/ZO/NS	NL/ZO/NS
NS	PM/NM/PL	PM/NM/NL	PS/NS/NS	PS/NS/NS	PS/NL/NM	PL/NL/NL	PL/ZO/ZO	ZO/PL/NS	NL/PL/NS
ec NL	PM/NM/PL	PM/NM/NL	PS/NS/NS	PL/NS/NS	PL/NL/NS	ZO/ZO/ZO	NL/PL/ZO	NL/PL/NL	NS/PS/NL
ZO	PM/NM/ZO	PS/NM/NL	PS/NS/NL	PL/NL/NL	ZO/ZO/NL	ZO/PL/PL	NL/PL/NS	NS/PS/ZO	NS/PS/ZO
PL	PS/NS/ZO	PS/NS/ZO	PL/NL/ZO	ZO/ZO/ZO	NL/PL/ZO	NL/PS/ZO	NS/PS/ZO	NS/PM/ZO	NM/PM/ZO
PS	PS/NS/PM	PL/NL/NS	ZO/ZO/PL	NL/PL/PL	NL/PL/PL	NS/PS/PL	NS/PS/PS	NM/PM/PS	NM/PM/PM
PM	PL/ZO/PM	ZO/ZO/PS	NL/PL/PS	NS/PS/PS	NM/PM/PS	NM/PM/PS	NM/PM/PM	NB/PB/PM	NB/PB/PB
PB	ZO/ZO/PB	ZO/ZO/PB	NS/PL/PM	NM/PS/PM	NM/PM/PM	NM/PM/PM	NB/PM/PM	NB/PB/PB	NB/PB/PB

TABLE 4. Road information segmented PID truth table.

$k_p/k_i/k_d$	Increments			
	ZO	PS	PM	PB
	ZO/ZO/ZO	NS/NS/ZO	NM/NS/ZO	NB/NM/ZO

purposes. The relevant parameters of the BP neural network are presented in Table 5. The final training and test set information, along with their classification results, are presented in Table 6, Figure 10 and Figure 11.

TABLE 5. BP neural network parameter table.

Number of features	Hidden layer neurons	Output layer class	The maximum number of iterations	Learning rate
9	6	4	10000	0.01

TABLE 6. The number of samples in training set and test set.

Road attributes	Asphalt road	short grass road	Tall grass road	Sandy road
The number of samples in the training set	26	16	19	19
Test set sample size	19	16	25	20

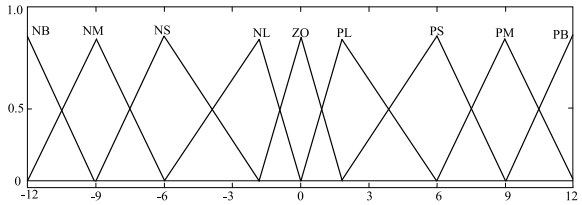

FIGURE 9. Membership function diagram.

The results are shown in Figure 10 and Figure 11. Figure 11 shows the results of multiple runs under the same neural network, where the results of the first run are depicted in detail, as shown in Figure 10. Each dot in the figure11 indicates the recognition result for a run of the program (the vertical coordinate indicates the number of runs and the horizontal coordinate indicates the road category), and the number after the dot indicates the recognition accuracy. The symbol "+" means that other categories were incorrectly classified as this category, and the symbol "−" means that this category was incorrectly classified as results of other categories.

In the process of verification, the high grass road has large fluctuation characteristics, resulting in large vehicle bump characteristics, which can greatly affect the change of attitude angle and motor speed. The method proposed in this paper can amplify the difference with the other three types of roads, which is easy to identify. The short grass road has small fluctuation characteristics, which has little impact on vehicle turbulence characteristics, but it also has certain turbulence characteristics, which can be well distinguished from other three types of roads by the method in Table 2. However, there is some confusion between sand road and asphalt road. The main reason is that the fluctuation of sand road and asphalt road is very small. The expression X_9 in Table 2 is mainly used to determine the difference between the two. As the material of sand road is soft, it is easy to cause big difference in the adhesion of tires at different positions. This error is within the allowable range of error, and the overall recognition rate reaches more than 98%, which will not affect the stability control of the later text greatly.

The method in this paper is compared with the road recognition methods given in literatures [14], [15], [16], [17], as is shown in Figure 12. This paper sampled the roll angle, pitch angle and rotation speed of the left and right wheel motor of the unmanned vehicle, and converted this information into 9 characteristic values input by the neural network. Compared with the methods given in other literatures, the increase of sampling information can enhance the anti-interference performance of the system. Using more sampling information and more features at the same time can effectively reduce the complexity of the algorithm [26] and ensure the real-time performance of the system. In recognition results, the recognition rate reaches 98%, higher than the other methods. In terms of the number of terrain categories, although [17] has identified 6 kinds of roads, these roads have large differences in the degree of undulation, and the sandy pavement with slight undulation and high slip rate have not been identified. Literature [16] can recognize 9 kinds of roads, including sandy pavement, but the method is to use the road's own attributes for recognition, and the recognition rate is only 80%. Meanwhile, it is difficult to select a reasonable on-board sensor for information extraction.

B. ADAPTED PID CONTROL RESULTS

Adapted PID control experiments are carried out on diverse road surfaces, utilizing the experimental vehicle presented in Table 1. The original PID parameters are obtained using the Ziegler-Nichols [27] tuning method, producing the speed loop parameters of $k_p = 120$, $k_i = 20$, and $k_d = 300$, and the current loop parameters of $k_p = 80$, $k_i = 28$, and $k_d = 100$. Subsequently, the adaptive parameters from Table 3 and Table 4 are added on the original PID to obtain the adaptive PID algorithm, which are employed in the four categories of roads in Figure 7.

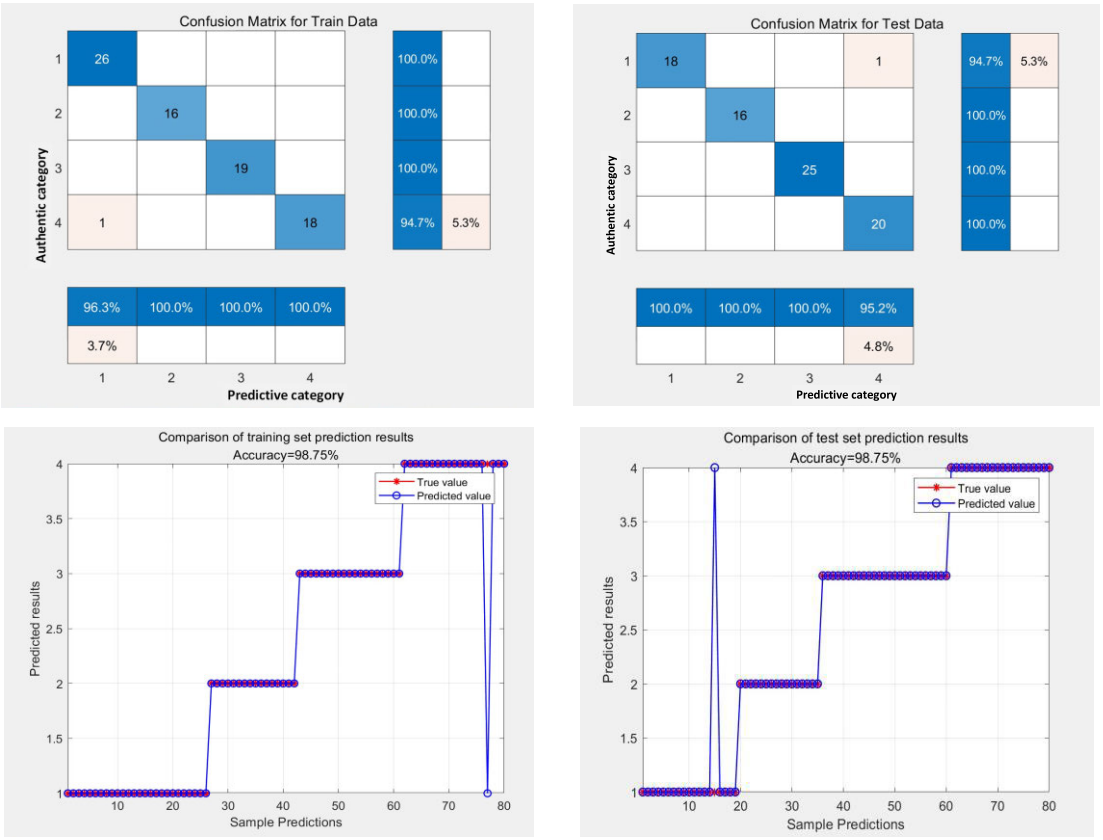

FIGURE 10. Results of neural network recognition (First run results).

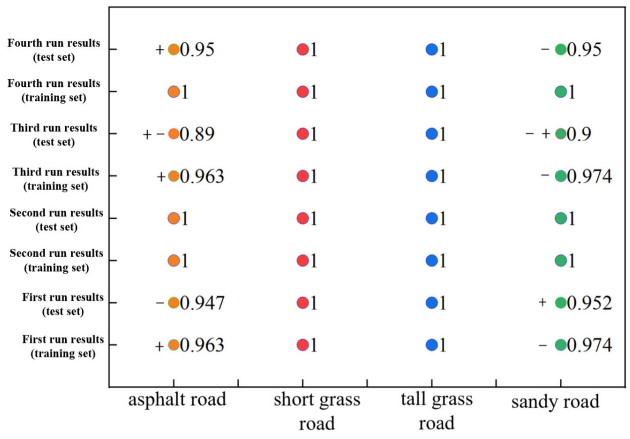

FIGURE 11. Results of neural network recognition (Results of four runs).

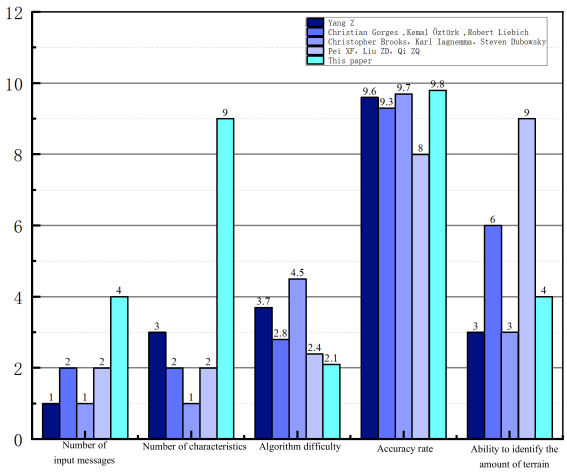

FIGURE 12. Comparison of relevant literature methods.

The adaptive PID algorithm used in this paper is compared with the original PID algorithm. The obtained speed and current curves are then illustrated in Figure 12. Figure a-d show the speed waveforms of the motor for the unmanned vehicle operating on the four road surfaces. Figure e-h show the current waveforms operating on the four road surfaces.

The experimental results are shown in Figure 13. As can be seen from the comparison in the figure a and e, if the algorithm in reference [27] is used only, there is not much difference between them and they can both have good setting effect under structured asphalt pavement. However, under unstructured pavement, the Ziegler-Nichols algorithm is weak in processing unstructured complex terrain due to the fixed PID parameters, so it cannot achieve a better setting effect. The adaptive PID algorithm in this paper can adjust

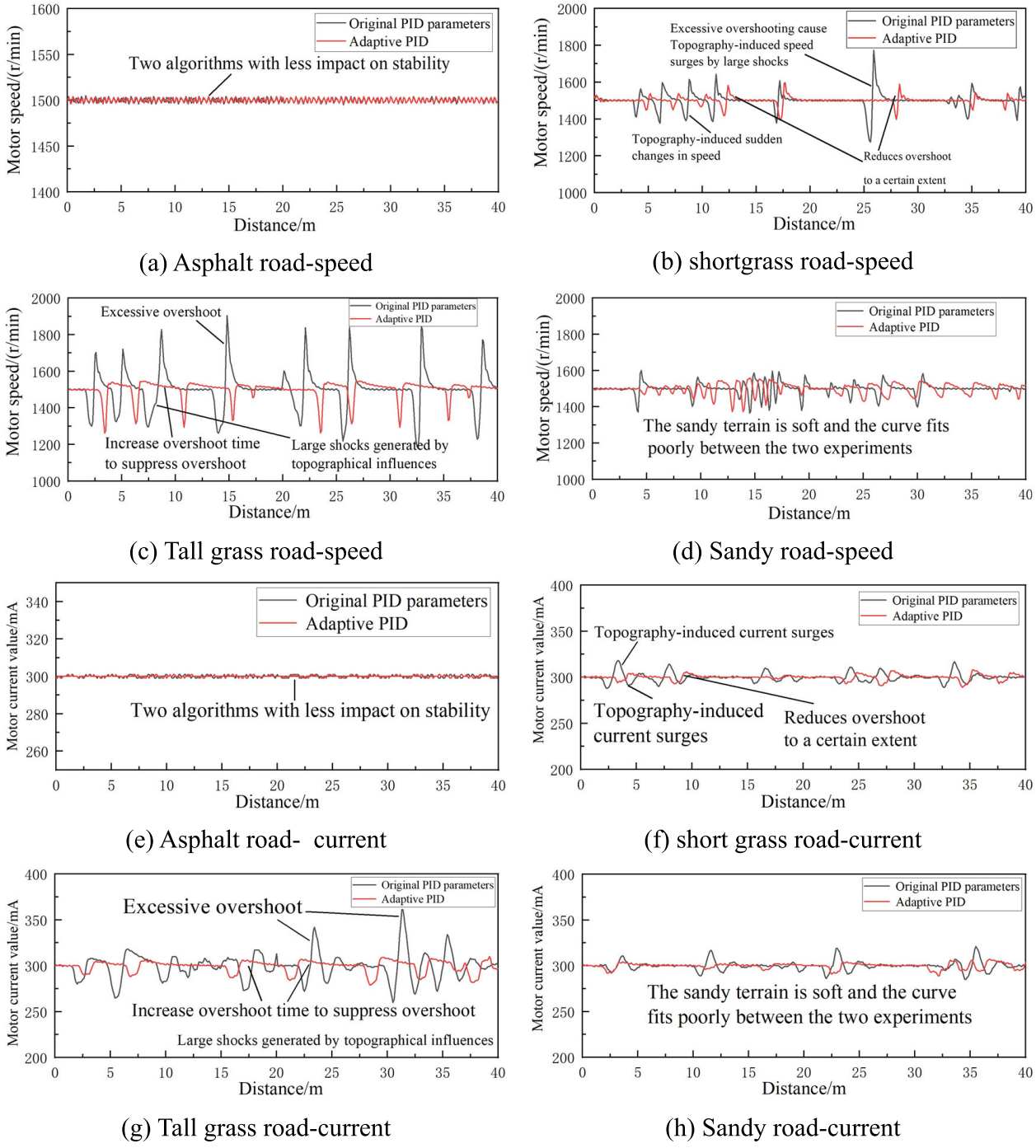

FIGURE 13. Real-time curves of vehicle motor current and rotational speed.

the PID parameters in real time according to the current road terrain characteristics.

Then, the curve generated by the adaptive PID parameters is further analyzed. When the value of k_p and k_i is large, the adjustment time can be effectively reduced, but it is easy to overshoot. At this time, k_d can be used to increase the system damping for vibration suppression. This paper compares the adaptive PID parameters studied with the original PID parameters. As can be seen from the figure, on the asphalt pavement, because the road is relatively flat, there is little difference between the original PID and adaptive PID algorithm of both current ring and speed ring on vehicle speed and motor torque. On short grass off-road road and high grass off-road road, due to the large ups and downs of the road, adaptive PID algorithm through the k_p and k_i value of the corresponding reduction, by sacrificing the adjustment time,

the motor output speed and torque vibration inhibition, can effectively enhance the stability of speed and torque, so that it will not overshooting.

Figures b and f show the velocity and current (torque) waveforms of the unmanned vehicle on a short grass off-road surface, with the velocity waveform producing a total of eight oscillations. When the original PID parameters were used for control, the average oscillation amplitude was between 1410-1563 (r/min) and the largest oscillation was the sixth oscillation, which was between 1274-1772 (r/min). The adaptive PID algorithm could limit the fluctuation range of the average oscillation amplitude to 1418-1528 (r/min) and the maximum oscillation amplitude to 1397-2588 (r/min). The current produced a total of 8 oscillations with an average oscillation amplitude between 291-312mA. After control by the adaptive algorithm, the average oscillation interval was limited to between 293-308mA and the maximum oscillation amplitude 287-318mA was limited to between 291-310mA.

Figure c and g show the speed and current (torque) waveforms of the unmanned vehicle on a high grass off-road surface. The speed waveform produces a total of eight oscillations, with the average oscillation amplitude of 1296-1828 (r/min) and the maximum oscillation being the fourth oscillation with an amplitude of 1186-1904 (r/min). Using the adaptive PID algorithm, the average speed oscillation can be limited to 1294-1537 (r/min) and the maximum speed oscillation amplitude is limited to 1276-1537 (r/min). As the road undulates when the unmanned vehicle is on a high grass off-road surface, which has a large impact on the motor current (torque), it is difficult to record the number of torque oscillations, so only the maximum motor current (torque) amplitude is analyzed and the maximum current oscillation amplitude is reduced from the original 260-361mA to 279-309 mA by the adaptive PID algorithm.

Figure d and h are waveforms of the unmanned vehicle driving on a sandy road surface. Since the sandy road surface material is soft and the terrain is extremely changeable, it is difficult to record the number of sudden changes in motor speed and current (torque) in the experiment, so only the maximum oscillation value amplitude of both is described. In the original PID algorithm, the maximum oscillation of speed was 1365-1597 (r/min), which was deducted to 1374-1556 (r/min) by the adaptive algorithm. In the original PID algorithm, the oscillation of the current (torque) is 285-321mA, while with the adaptive algorithm, the oscillation is suppressed to 291-306 mA.

According to the above analysis, the method proposed in this paper can enhance the stability of the vehicle under different road surfaces.

V. CONCLUSION

There are two main problems addressed in this paper, that is, how to identify the road attributes of the current driving of the unmanned vehicle and how to establish a reasonable control method according to the road attributes currently identified. Therefore, the main contributions of this paper can be summarized as follows:

(1) Considering the poor real-time and weak anti-interference performances and limited road recognition ability of a single sensor, this paper proposes to sample the roll angle and pitch angle of the unmanned vehicle driving on different roads by gyroscope sensors (IMU), recording the shaking information. The speed information of the left and right wheels is sampled through the motor speed sensor (motor encoder), recording the driving status of the unmanned vehicle. In this way, not only the off-road pavement with large fluctuation can be identified, but also the sandy pavement with small fluctuation and high slip rate can be well identified, with the overall recognition rate reaching 98%.

(2) A multi-loop adaptive PID control system is proposed. The system uses the speed loop as the outer loop and the torque loop (current loop) as the inner loop. The fuzzy PID algorithm is used for the speed loop and for the torque loop, the segmented PID algorithm is utilized to achieve the effect of stable driving on different road surfaces.

The feasibility and effectiveness of the stability control method for vehicles operating on unstructured roads, as proposed in this study, have been demonstrated. Furthermore, the increasing focus on unstructured surfaces in future smart agriculture and military technology highlights the importance of developing effective motion control methods for UGVs. Therefore, this research provides a foundation for further studies on UGV motion control on unstructured roads. However, some limitations should be noted, primarily in two aspects:

(1) Currently, the road recognition results are solely employed in the current loop for motor torque control, which has produced particularly noticeable effect. In future studies, the road attributes can be applied to speed control, enabling the implementation of diverse speed limits for different road surfaces to ensure secure and stable traversal of off-road terrains by the vehicles.

(2) To enhance the clarity of the experimental results, the test vehicle used in this study did not utilize a suspension system for mechanical damping. In real-world engineering projects, independent suspension systems are extensively adopted. Therefore, in future research, mechanical damping can be combined with the aforementioned motor control damping to conduct an integrated analysis and determine the optimal control method.

ACKNOWLEDGMENT

The authors would like to thank the coordinating editor and the anonymous reviewers for very useful and constructive feedback.

REFERENCES

[1] J. A. Whitson, D. Gorsich, V. V. Vantsevich, M. Letherwood, O. Sapunkov, and L. Moradi, "Military unmanned ground vehicle maneuver: A review and formulation," SAE Tech. Paper 2023-01-0108, 2023, doi: 10.4271/2023-01-0108.

[2] J. Kim, S. Kim, C. Ju, and H. I. Son, "Unmanned aerial vehicles in agriculture: A review of perspective of platform, control, and applications," *IEEE Access*, vol. 7, pp. 105100–105115, 2019.
[3] A. D. Boursianis, M. S. Papadopoulou, P. Diamantoulakis, A. Liopa-Tsakalidi, P. Barouchas, G. Salahas, G. Karagiannidis, S. Wan, and S. K. Goudos, "Internet of Things (IoT) and agricultural unmanned aerial vehicles (UAVs) in smart farming: A comprehensive review," *Internet Things*, vol. 18, May 2022, Art. no. 100187.
[4] S. Park and Y. Choi, "Applications of unmanned aerial vehicles in mining from exploration to reclamation: A review," *Minerals*, vol. 10, no. 8, p. 663, Jul. 2020.
[5] V. Shuts and A. Shviatsova, *ICCPT 2019: Current Problems of Transport: Proceedings of the 1st International Scientific Conference, May 28–29, 2019, Ternopil, Ukraine/Ternopil Ivan Puluj National Technical University*. Ternopil, Ukraine: TNTU, 2019, pp. 174–184.
[6] X. Yang, X. Yan, W. Liu, H. Ye, Z. Du, and W. Zhong, "An improved Stanley guidance law for large curvature path following of unmanned surface vehicle," *Ocean Eng.*, vol. 266, Dec. 2022, Art. no. 112797.
[7] W. Chundi, "Area of the unstructured road detection based on machine vision and type identification," Dept. Automot. Eng., Jilin Univ., 2021, doi: 10.27162/d.cnki.Gjlin.2021.001377.
[8] U. Graf, P. Borges, E. Hernández, R. Siegwart, and R. Dubé, "Optimization-based terrain analysis and path planning in unstructured environments," in *Proc. Int. Conf. Robot. Autom. (ICRA)*, May 2019, pp. 5614–5620.
[9] L. Ying, "Surface morphology structure light measurement system calibration technology research," Dept. Electron. Eng., Xi'an Univ. Technol., 2021, doi: 10.27391/d.cnki.Gxagu.2021.000305.
[10] S. Yuze, "Global path planning and track tracking of unmanned wheeled vehicles on off-road pavement," Dept. Automot. Eng., Jilin Univ., 2020, doi: 10.27162/d.cnki.Gjlin.2020.006056.
[11] Z. Zhang, R. Ma, L. Wang, and J. Zhang, "Novel PMSM control for antilock braking considering transmission properties of the electric vehicle," *IEEE Trans. Veh. Technol.*, vol. 67, no. 11, pp. 10378–10386, Nov. 2018.
[12] P. Toivanen, V. Imani, and K. Haataja, "Three main paradigms of simultaneous localization and mapping (SLAM) problem," in *Proc. 10th Int. Conf. Mach. Vis. (ICMV)*, Apr. 2018, pp. 442–450.
[13] T. Lemaire, C. Berger, I.-K. Jung, and S. Lacroix, "Vision-based SLAM: Stereo and monocular approaches," *Int. J. Comput. Vis.*, vol. 74, no. 3, pp. 343–364, Jul. 2007.
[14] Y. Zhen, "Research on autonomous speed planning method of unmanned vehicle based on intelligent learning on complex road surface," Dept. Inf. Sci. Eng., Northeastern Univ., doi: 10.27007/d.cnki.gdbeu.2018.001301.
[15] C. A. Brooks and K. Iagnemma, "Vibration-based terrain classification for planetary exploration rovers," *IEEE Trans. Robot.*, vol. 21, no. 6, pp. 1185–1191, Dec. 2005.
[16] P. Xiaofei, L. Zhaodu, and Q. Zhiquan, "Road surface recognition method of vehicle longitudinal integrated control system," *China J. Highway Transp.*, vol. 27, no. 5, pp. 177–182, 2014, doi: 10.19721/J.CNKI.1001-7372.2014.05.013.
[17] C. Gorges, K. Öztürk, and R. Liebich, "Impact detection using a machine learning approach and experimental road roughness classification," *Mech. Syst. Signal Process.*, vol. 117, pp. 738–756, Feb. 2019.
[18] H. Yuhui, W. Xu, and H. Jiaming, "Review of UGV technology in off-road environment," *J. Beijing Inst. Technol.*, vol. 41, no. 11, pp. 1137–1144, 2021, doi: 10.15918/J.TBIT1001-0645.2020.144.
[19] Y. Wang, X. Zhao, S. Li, B. Su, and J. Gao, "Path tracking of eight in-wheel-driving autonomous vehicle: Controller design and experimental results," in *Proc. IEEE Int. Conf. Unmanned Syst. (ICUS)*, Oct. 2019, pp. 672–677.
[20] I. S. Leal, C. Abeykoon, and Y. S. Perera, "Design, simulation, analysis and optimization of PID and fuzzy based control systems for a quadcopter," *Electronics*, vol. 10, no. 18, p. 2218, Sep. 2021.
[21] S. Arof, M. S. Said, N. H. N. Diyanah, N. M. Noor, J. A. Jalil, P. Mawby, H. Arof, and E. Noorsal, "Series motor four-quadrant DC chopper: Reverse mode, direct current control, triple cascade PIDs, and ascend-descend algorithm with feedback optimization for automatic reverse parking," in *Progress in Engineering Technology II*. Cham, Switzerland: Springer, 2020, pp. 137–150.
[22] J. Meihui, Li Lijuan, and R. Jiaojiao, "PSO-BP neural network recognition for terahertz detection signals of multi-bonded defects," *ACTA Photonica Sinica*, vol. 50, no. 9, 2021, Art. no. 0930004, doi: 10.3788/GZXB20215009.0930004.
[23] Y. Ming and S. Weifeng, "Fault extraction of ship power system under load motor fault," *China Navigat.*, vol. 2015, no. 1, pp. 22–27, 2015.
[24] C. Ming, H. Bian, and Li Jing, "Research on voice print recognition technology of hydropower unit," *Elect. Technol.*, vol. 18, pp. 28–30, Jan. 2022.
[25] J. Peng, "A biomimetic very low frequency (VLF) active electrolocation system based on FFT feature extraction localization algorithm," *J. Mech. Eng.*, vol. 52, no. 2, p. 157, 2016, doi: 10.3901/JME.2016.02.157.
[26] A. Benoit, Y. Robert, and F. Vivien, *A Guide to Algorithm Design: Paradigms, Methods, and Complexity Analysis*. Boca Raton, FL, USA: CRC Press, 2013.
[27] I. P. Canal, M. M. P. Reimbold, and M. de Campos, "Ziegler–Nichols customization for quadrotor attitude control under empty and full loading conditions," *Comput. Model. Eng. Sci.*, vol. 125, no. 1, pp. 65–75, 2020.

XIANG AO was born in Hubei, China, in 1997. He is currently pursuing the master's degree in control engineering with the Naval University of Engineering. His current research interest includes the motion control of unmanned vehicles on unstructured roads.

LI-MING WANG was born in 1978. He is currently a Professor, a Doctoral Supervisor, and a Chief Scientist of the National Key Research and Development Program. He is an expert in the fields of intelligent equipment and unmanned platforms. He developed devices for power fault recording, harmonic monitoring, and centralized power monitoring have been equipped for military applications. As the lead author, he has published nine books and textbooks and more than 60 articles and searched for more than 20 articles through SCI/EI. He led one National Key Research and Development Project and also led/participated in two projects funded by the National Natural Science Foundation of China and more than 20 projects related to military pre-research, internal scientific research, and maintenance programs. He received four national invention patents, ten utility model patents, and ten software copyrights. His current research interests include ship intelligent monitoring technology, intelligent detection robots, and autonomous robots. The target audience for cultivating high-tech innovative talents in the Navy, third batch of young and middle-aged subject leaders in the Naval University of Engineering, 33511 talent training targets, and off-campus doctoral supervisors in the field of electronics and information engineering at the Beijing Institute of Technology. He received three awards from the Military Scientific and Technological Progress.

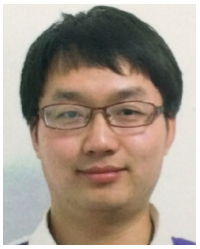

JIA-XIN HOU received the Ph.D. degree in control science and engineering from Harbin Engineering University, in 2020. Currently, he is with the Teaching and Research Section of Control Engineering, Naval University of Engineering. He is mainly teaching courses on the principles of automatic control and intelligent control. His current research interests include signal processing, information fusion, navigation guidance and control, object tracking, and visual object tracking.

YU-QUAN XUE was born in Jiangsu, China, in 1993. He received the B.S. degree from Yangzhou University, in 2016, and the M.S. degree from the Shanghai Institute of Technology, in 2020. His current research interest includes the dynamics and control of autonomous systems.

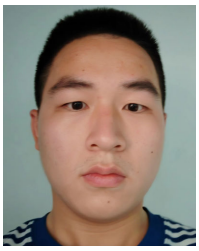

SHANG-JUN RAO was born in Hubei, China, in 2002. He is currently pursuing the bachelor's degree with the Naval University of Engineering. His current research interest includes electrical engineering and its automation.

ZI-YANG ZHOU was born in Hunan, China, in 1999. He received the bachelor's degree from the Hunan University of Technology, in 2021. He is currently pursuing the master's degree in electronic information with the Naval University of Engineering.

FU-XUE JIA was born in Hubei, China, in 2001. He is currently a Junior Cadet with the Naval University of Engineering. His current research interest includes wireless communications.

ZHI-YUAN ZHANG was born in Qingdao, Shandong, in October 2001. He is currently pursuing the degree in marine engineering with the College of Power Engineering, Naval University of Engineering. He has won many national competition awards.

LONG-MEI LI was born in Hubei, China, in 1989. She received the B.S., M.S., and Ph.D. degrees from the National University of Defense Technology, China, in 2011, 2013, and 2018, respectively. She is currently a Lecturer with the Naval University of Engineering. Her current research interests include evolutionary computation and intelligent control.